

Helioseismology: a fantastic tool to probe the interior of the Sun

Maria Pia Di Mauro

Teoretisk Astrofysik Center, Bygn. 520, Ny Munkegade, DK 8000 Aarhus C, Denmark

Abstract. Helioseismology, the study of global solar oscillations, has proved to be an extremely powerful tool for the investigation of the internal structure and dynamics of the Sun.

Studies of time changes in frequency observations of solar oscillations from helioseismology experiments on Earth and in space have shown, for example, that the Sun's shape varies over solar cycle timescales.

In particular, far-reaching inferences about the Sun have been obtained by applying inversion techniques to observations of frequencies of oscillations. The results, so far, have shown that the solar structure is remarkably close to the predictions of the standard solar model and, recently, that the near-surface region can be probed with sufficiently high spatial resolution as to allow investigations of the equation of state and of the solar envelope helium abundance.

The same helioseismic inversion methods can be applied to the rotational frequency splittings to deduce with high accuracy the internal rotation velocity of the Sun, as function of radius and latitude. This also allows us to study some global astrophysical properties of the Sun, such as the angular momentum, the gravitational quadrupole moment and the effect of distortion induced on the surface (oblateness).

The helioseismic approach and what we have learnt from it during the last decades about the interior of the Sun are reviewed here.

1 Introduction

In the early 60's accurate observations of the photospheric spectrum revealed the existence of oscillatory motions, with periods around 5 minutes, on the Sun's surface [63], [68]. The observed oscillatory character of the surface was theoretically explained by Ulrich [92] and independently by Leibacher & Stein [62] as due to acoustic waves (i.e. p -modes) – generated for some not well known reason in the convection zone and maintained by pressure force – trapped in resonant cavities between the Sun's surface and an inner turning point, whose depth depends on the local speed of sound and frequency. Only few years later more accurate observations carried out by Deubner [28] were able to confirm the previous theoretical hypothesis about the modal nature of solar oscillations.

The unprecedented discovery of existence of such phenomenon opened for the first time human eyes to the knowledge of the solar interior and formed the basis for the development of *helioseismology*. Like the geoseismology, which studies the Earth's interior through the waves produced during the earthquakes, helioseismology study the interior of the Sun through the small oscillations detected at the surface.

In fact, since each wave, characterized by a specific frequency and wave number, propagates through a different region of the Sun, probing the physical properties of the crossed medium, like temperature and composition, it is possible to deduce the internal stratification and dynamics of the Sun from the spectrum of resonant modes.

Since the first observations, many thousands of modes of oscillation have already been identified with great accuracy. The spectrum extends from 0.6 *mHz* to 5.5 *mHz* and it has a maximum amplitude of about 15 *cm/s* in velocity. This incredible amount of information collected contributed to the success of this discipline and has permitted a deep knowledge of the Sun, not imaginable thirty years ago.

2 Theoretical approach to helioseismology

2.1 Basic equations of adiabatic oscillations

A star, like the Sun, is a gaseous sphere in hydrostatic equilibrium, and the oscillations are fluid-dynamical phenomena caused by the action of a restoring force which arises when the original equilibrium status is perturbed. Such hydrodynamical systems can be described by specifying all the physical quantities as functions of the position \mathbf{r} and time t .

To provide a background for the treatment of stellar pulsations, it is useful to consider briefly the basic equations of hydrodynamics, which can be derived by applying the fundamental principles of conservation of mass, of momentum and of energy. We neglect viscosity and magnetic fields and we can also assume that gravity is the only acting body force and that the radiation is the dominant contribution to the flux of energy.

The conservation of mass is expressed by the equation of continuity:

$$\frac{d\rho}{dt} = -\rho \operatorname{div} \mathbf{v} , \quad (1)$$

where $\rho = \rho(\mathbf{r}, t)$ is the density and $\mathbf{v} = d\mathbf{r}/dt$ is the local velocity. The equation of motion is:

$$\rho \frac{d\mathbf{v}}{dt} = -\nabla p + \rho \nabla \Phi , \quad (2)$$

where $p = p(\mathbf{r}, t)$ is the pressure and Φ is the gravitational potential which satisfies the Poisson's Equation,

$$\nabla^2 \Phi = -4\pi G \rho , \quad (3)$$

G being the gravitational constant. And finally the energy equation:

$$\frac{dQ}{dt} = \frac{dE}{dt} + p \frac{d}{dt} \left(\frac{1}{\rho} \right) = \varepsilon - \frac{\operatorname{div} \mathbf{F}}{\rho} , \quad (4)$$

where dQ/dt is the rate of heat loss or gain per unit of mass, E is the internal energy in unit of mass, ε is the rate of energy generation per unit mass, while \mathbf{F} is the flux of energy.

By using thermodynamic identities the energy equation can be expressed in terms of other, more convenient variables, like in [24]:

$$\frac{dQ}{dt} = \frac{1}{\varrho(\Gamma_3 - 1)} \left(\frac{dp}{dt} - \frac{\Gamma_1 p}{\varrho} \frac{d\varrho}{dt} \right), \quad (5)$$

where Γ_1 and Γ_3 are the first and the third adiabatic exponent, defined by:

$$\Gamma_1 = \left(\frac{\partial \ln p}{\partial \ln \varrho} \right)_{ad}, \Gamma_3 - 1 = \left(\frac{\partial \ln T}{\partial \ln \varrho} \right)_{ad}, \quad (6)$$

where T is the temperature and the derivatives are calculated at constant specific entropy.

The observed amplitude of solar oscillations are very small ($\delta r/R_\odot \simeq 10^{-4}$), so that the pulsations can be described with accuracy by applying a linear perturbation analysis of the basic equations of hydrodynamic.

Let us consider a static equilibrium model with pressure $p_0(r)$, density $\varrho_0(r)$ etc. If we consider *Eulerian* perturbations, the generic physical quantity f can be written in the following way:

$$f(\mathbf{r}, t) = f_0(\mathbf{r}) + f'(\mathbf{r}, t), \quad (7)$$

where $f_0(\mathbf{r})$ is the unperturbed term and $f'(\mathbf{r}, t)$ is the small perturbation at a given spatial point. The small perturbation can also be written in the Lagrangian form, by considering a frame following the motion of an element of gas which moves from position \mathbf{r} to $\mathbf{r} + \delta \mathbf{r}$:

$$\delta f(\mathbf{r}) = f(\mathbf{r} + \delta \mathbf{r}) - f_0(\mathbf{r}) = f'(\mathbf{r}) + \delta \mathbf{r} \cdot \nabla f_0. \quad (8)$$

Since the typical pulsation period is much smaller than the time required to dissipate the thermal energy, we first assume that the adiabatic approximation is sufficient to discuss the dynamical characteristics in the interior of the Sun. This hypothesis, which greatly simplifies the treatment of stellar pulsations, is not longer verified in the very superficial layers and nonadiabatic effects on the frequencies should not be neglected in the study of the surface layers and of the pulsation energetics.

According to these assumptions and by perturbing the four basic equations (1)–(4), we obtain the following system of four linear equations in four unknowns to study the small oscillations under adiabatic conditions:

$$\varrho' = -\operatorname{div}(\varrho_0 \delta \mathbf{r}), \quad (9a)$$

$$\varrho_0 \frac{\partial \mathbf{v}}{\partial t} = -\nabla p' + \varrho' \nabla \Phi + \varrho_0 \nabla \Phi', \quad (9b)$$

$$\nabla^2 \Phi' = -4\pi G \varrho', \quad (9c)$$

$$p' + \delta \mathbf{r} \cdot \nabla p_0 = \frac{\Gamma_1 p_0}{\varrho_0} (\varrho' + \delta \mathbf{r} \cdot \nabla \varrho_0). \quad (9d)$$

An extensive and detailed derivation of the equations of adiabatic oscillations is provided by Unno et al. in [93], by Christensen–Dalsgaard & Berthomieu in [17] or by Christensen–Dalsgaard in [16].

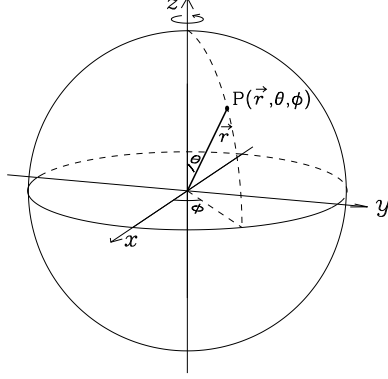


Fig. 1. The spherical polar coordinate system

2.2 Spherical Harmonic Representation

The general equations for small oscillations presented above must now be derived in the specific case of stars, which are assumed to have a spherically symmetric and a time-independent equilibrium structure.

Let consider a spherical polar coordinates system (r, θ, ϕ) , where r is the distance to the centre, θ is the colatitude, and ϕ is the longitude (Fig. 1). In the polar coordinates system a vector field can be written by specifying its components in the radial and angular directions. Thus the displacement, for example, can be written as:

$$\delta \mathbf{r}(r, \theta, \phi, t) = \xi_r \mathbf{a}_r + \xi_\theta \mathbf{a}_\theta + \xi_\phi \mathbf{a}_\phi, \quad (10)$$

where \mathbf{a}_r , \mathbf{a}_θ and \mathbf{a}_ϕ are the unit vectors in the r , θ and ϕ directions respectively. By introducing ξ_h , the horizontal component of the vector, we can also write:

$$\delta \mathbf{r} = \xi_r \mathbf{a}_r + \xi_h \mathbf{a}_h, \quad (11)$$

where $\xi_r = \xi_r(r, \theta, \phi, t)$ and $\xi_h = \xi_h(r, \theta, \phi, t)$ are the radial and horizontal components of the displacement.

Since the equilibrium state depends only on the radius r , the solutions of the linear system (9a)–(9d) can be obtained in the following form, by separating the spatial from the temporal dependence:

$$f'(r, \theta, \phi, t) = \tilde{f}'(r) f(\theta, \phi) \exp(-i\omega t), \quad (12)$$

where the time dependence has been expressed in terms of an harmonic function, characterized by a frequency ω , the amplitude $\tilde{f}'(r)$ is a function of r alone, and $f(\theta, \phi)$ describes the angular variation of the solution.

In the spherical symmetric system, all derivatives with respect to θ and ϕ can be expressed in the form of the tangential Laplace operator:

$$\nabla_h^2 \equiv \frac{1}{r^2 \sin \theta} \frac{\partial}{\partial \theta} \left(\sin \theta \frac{\partial}{\partial \theta} \right) + \frac{1}{r^2 \sin^2 \theta} \frac{\partial^2}{\partial \phi^2}. \quad (13)$$

Consequently, $f(\theta, \phi)$ can be found as eigenfunction of ∇_h^2 and it may be chosen to be the spherical harmonic $Y_l^m(\theta, \phi)$ of degree l and azimuthal order m , which indeed satisfies the eigenvalues problem:

$$\nabla_h^2 Y_l^m(\theta, \phi) = -\frac{l(l+1)}{r^2} Y_l^m(\theta, \phi) = -k_h^2 Y_l^m(\theta, \phi), \quad (14)$$

where l and m are integers, such that $-l \leq m \leq l$, and k_h is the horizontal component of the wave number. The spherical harmonics $Y_l^m(\theta, \phi)$ are defined by:

$$Y_l^m(\theta, \phi) = N_{m,l} P_l^m(\cos \theta) e^{im\phi}, \quad (15)$$

where P_l^m is the associated Legendre polynomial and $N_{m,l}$ is a constant such that the following integral over the unit sphere is satisfied:

$$\int_0^{2\pi} \int_0^\pi Y_l^m(\theta, \phi) Y_{l'}^{m'}(\theta, \phi) \sin \theta d\theta d\phi = \delta_{ll'} \delta_{mm'}, \quad (16)$$

where $\delta_{ll'}$ and $\delta_{mm'}$ are Kronecker's deltas, so that the integral is zero if $l \neq l'$ and $m \neq m'$.

It follows that the perturbation quantities (12) can be written as:

$$f'(\mathbf{r}, \theta, \phi, t) = \sqrt{4\pi} \tilde{f}'(r) Y_l^m(\theta, \phi) e^{-i\omega t} \quad (17)$$

and that the displacement vector can be expressed by:

$$\delta \mathbf{r} = \sqrt{4\pi} \Re \left\{ \left[\tilde{\xi}_r(r) \mathbf{a}_r + \tilde{\xi}_h(r) \left(\frac{\partial}{\partial \theta} \mathbf{a}_\theta + \frac{\partial}{\sin \theta \partial \phi} \mathbf{a}_\phi \right) \right] Y_l^m(\theta, \phi) e^{-i\omega t} \right\}, \quad (18)$$

where \Re stands for the real part.

By substituting the spherical harmonic representations into Eqs. (9a)–(9d), we obtain the following set of ordinary differential equations, which describes the stellar adiabatic oscillations:

$$\frac{d\xi_r}{dr} = -\left(\frac{2}{r} + \frac{1}{\Gamma_1 p} \frac{dp}{dr}\right) \xi_r + \frac{1}{\varrho c^2} \left(\frac{S_l^2}{\omega^2} - 1\right) p' - \frac{l(l+1)}{r^2 \omega^2} \Phi', \quad (19a)$$

$$\frac{dp'}{dr} = \varrho(\omega^2 - N^2) \xi_r + \frac{1}{\Gamma_1 p} \frac{dp}{dr} p' + \varrho \frac{d\Phi'}{dr}, \quad (19b)$$

$$\frac{1}{r^2} \frac{d}{dr} \left(r^2 \frac{d\Phi'}{dr} \right) = -4\pi G \left(\frac{p'}{c^2} + \frac{\varrho \xi_r}{g} N^2 \right) + \frac{l(l+1)}{r^2} \Phi', \quad (19c)$$

where S_l is the Lamb frequency

$$S_l^2 = \frac{l(l+1)c^2}{r^2}, \quad (20)$$

N is the buoyancy frequency

$$N^2 = g \left(\frac{1}{\Gamma_1 p} \frac{dp}{dr} - \frac{1}{\varrho} \frac{d\varrho}{dr} \right), \quad (21)$$

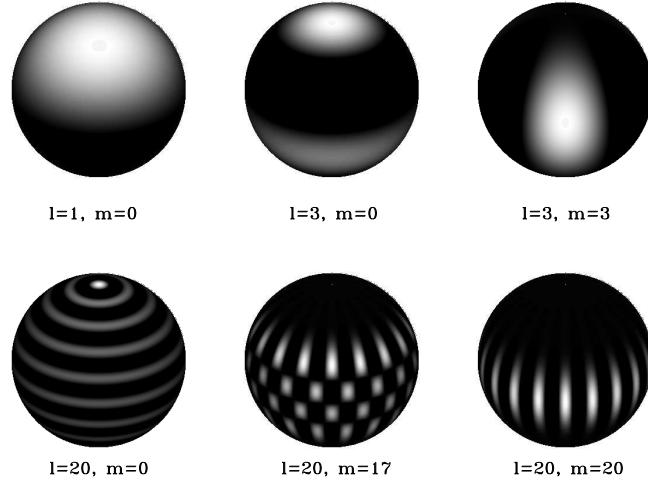


Fig. 2. Illustration of some spherical harmonics. For clarity the polar axis has been rotated of 30° into respect the plane of the page. Positive patterns are indicated by brighter surfaces while negative patterns are darker

and c is the speed of the sound in adiabatic conditions, such that under the reasonable assumption that the stellar interior can be approximate to an ideal gas:

$$c^2 = \frac{\Gamma_1 p}{\varrho} \simeq \frac{\Gamma_1 k_B T}{\mu m_u}, \quad (22)$$

where k_B is the Boltzmann's constant, μ is the mean molecular weight and m_u is the atomic mass unit.

The fourth-order system of ordinary differential equations (19a)–(19c), together with appropriate boundary conditions at centre $r = 0$ and at the surface $r = R_\odot$, constitutes an eigenvalue problem, which admits solutions only for particular values of the eigenfrequencies ω . The discrete set of solutions, obtained for each (l, m) is labelled with an integer n and describes the so-called *spheroidal modes*. The modes are therefore identified by three quantum numbers, the radial order n , which is the number of the nodes of the wave in the radial direction, the harmonic degree l , which is the number of nodes on the surface in the direction of the latitude and the azimuthal order m , which specifies the number of the nodes along the longitude on the surface. A few examples of spherical harmonics are shown in Fig. 2. It should be noticed, that in the case of spherical symmetry there are not preferential directions on the sphere, therefore the modes show $(2l + 1)$ -fold degeneracy in m and both the eigenfrequencies and the eigenfunctions do not depend on m .

3 Propagation of solar oscillations

It can be noticed that the set of equations of adiabatic oscillations (19a)–(19c) can be easily solved, once the boundary conditions are known. However, an accurate interpretation of the results requires a more complete description of the phenomenon. This can be obtained by an asymptotic analysis of the pulsation equations, justified by the fact that the acoustic modes observed in the Sun, show fairly high radial order and high degree.

The asymptotic analysis is usually carried out in the Cowling approximation [23], by neglecting the perturbation Φ' of the gravitational potential. In this case the oscillations equations (19a)–(19c) reduce to a second-order system, that according to [29] it can be written in the following approximate expression:

$$\frac{d^2\Psi}{dr^2} + \frac{1}{c^2} \left[\omega^2 - \omega_c^2 - S_l^2 \left(1 - \frac{N^2}{\omega^2} \right) \right] \Psi = 0 , \quad (23)$$

where

$$\Psi(r) = c^2 \varrho^{1/2} \text{div} \delta \mathbf{r} . \quad (24)$$

The acoustical cut-off frequency ω_c is defined by:

$$\omega_c^2 = \frac{c^2}{4H^2} \left(1 - 2 \frac{dH}{dr} \right) , \quad (25)$$

where $H = -(\text{d} \ln \varrho / \text{d} r)^{-1}$ is the density scale height.

In a star in which the main body forces acting are the pressure and the gravity, two kind of oscillations can be maintained: the pressure or acoustic waves and the internal gravity waves, which form the classes of p modes and g modes respectively. The dispersion relation which describes the acoustic and gravity waves propagation in a medium, can be derived from Eq. (23) as:

$$c^2 k_r^2 = \omega^2 - \omega_c^2 - S_l^2 \left(1 - \frac{N^2}{\omega^2} \right) , \quad (26)$$

where k_r is the radial component of the wave number, which clearly depends on the variation of the characteristic frequencies S_l , N and ω_c with radius.

The propagation of modes of oscillation requires that $k_r^2 > 0$:

$$\omega^2 - \omega_c^2 - S_l^2 \left(1 - \frac{N^2}{\omega^2} \right) > 0. \quad (27)$$

It follows that the Eq. (27) is satisfied in the two domains where:

$$\omega^2 > S_l^2 \quad \omega^2 > \omega_c^2 \quad (28)$$

and

$$\omega^2 < N^2 . \quad (29)$$

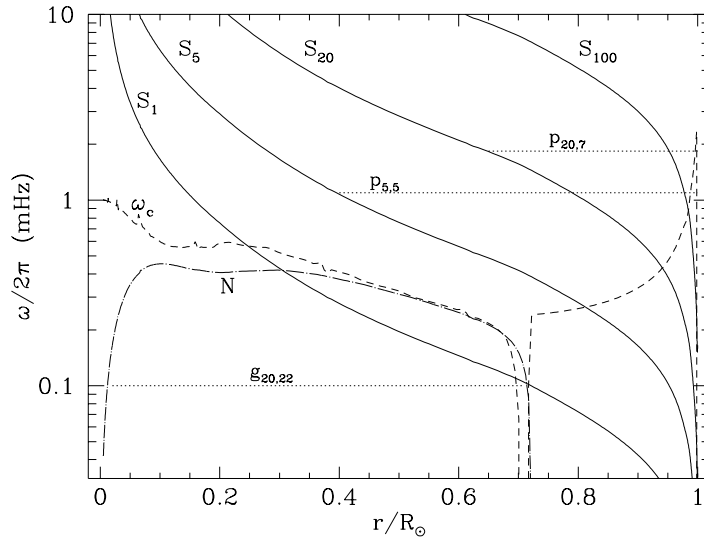


Fig. 3. Propagation diagram of the characteristic frequencies N , ω_c and S_l , calculated for some values of l , as functions of the fractional radius for a standard solar model. The horizontal lines indicate the trapping regions for a g mode with $l = 20$ and $n = 22$, and two p modes with $(l = 5, n = 5)$ and $(l = 20, n = 7)$

The conditions (28) and (29) define the *trapping regions* of p modes and g modes respectively, as illustrated in Fig. 3. Outside these regions the waves are evanescent and do not show oscillatory character in space and their amplitude decays exponentially.

Detection of g modes would be extremely valuable since they have highest amplitudes in the core, and hence their frequencies, if detected, should be very sensitive to the structure and rotation of the deeper interior of the Sun. Unfortunately, although claims for detection of g modes have been made [44], we still not have any confirmation that they are really excited in the Sun, and the observed five-minutes oscillations correspond only to p and f modes. Figure 4 shows a set of p modes frequencies obtained in 1996 [75] by the MDI [82] instrument on board the SOHO satellite.

The f modes correspond approximately to surface gravity waves with the condition that $\text{div}(\delta \mathbf{r}) \simeq 0$, so that according to Eqs. (9a)–(9d), it is possible to assume that $\delta p \simeq \delta \varrho \simeq 0$. The dispersion relation of the f modes is:

$$\omega^2 \simeq g_{\odot} k_h, \quad (30)$$

where $g_{\odot} = GM/R_{\odot}^3$. Thus, frequencies depend only on the mean density of the star, but not on its detailed internal structure.

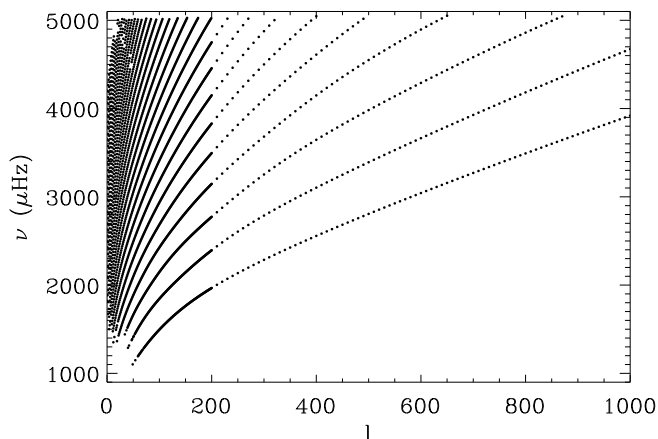


Fig. 4. A set of p-mode frequencies [75], as function of l , obtained by MDI instrument on board of SOHO. Each ridge contains modes with equal values of n

3.1 Properties of the acoustic modes

The propagation of p modes in the interior of the Sun can be interpreted very simply in geometrical terms, by studying the behaviour of rays of sound, as illustrated in Fig. 5. Locally the acoustic modes can be approximated by plane sound waves whose dispersion relation is:

$$\omega^2 = c^2 |\mathbf{k}|^2 = c^2 (k_r^2 + k_h^2), \quad (31)$$

where k_r and k_h are the radial and horizontal components of the wave vector \mathbf{k} . This means that the properties of the modes are entirely controlled by the variation of the adiabatic sound speed c , which depends on temperature (Eq. 22). From Eq. (31), by using the definition of k_h given in Eq. (14), it follows that:

$$k_r^2 = \frac{\omega^2}{c^2} - \frac{l(l+1)}{r^2} = \frac{\omega^2}{c^2} \left(1 - \frac{S_l^2}{\omega^2} \right). \quad (32)$$

At the surface, where c is small, k_r is large and hence the wave propagates almost vertically. Due to the increase of the sound speed with temperature, k_r decreases with depth, while k_h increases as r decreases, until $k_r = 0$ and the wave travels mostly horizontally. This condition is reached at the turning point r_t , where:

$$\frac{c(r_t)}{r_t} = \frac{\omega}{\sqrt{l(l+1)}}. \quad (33)$$

At the turning point, the wave is gradually refracted and goes back towards the surface. For $r < r_t$, k_r is imaginary and the wave decays exponentially.

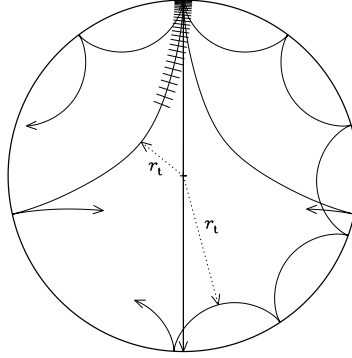


Fig. 5. Propagation of rays of sound in the solar interior in the case of two p modes with degrees $l = 5$ and $l = 15$. The acoustic waves are reflected at the surface owing to the rapid decrease of density, and at the inner turning point r_t due to the increase of the temperature with depth. Notice that waves with a smaller wavelength corresponding to a higher value of the degree l , penetrate less deeply

It appears clear from the Eq. (33) that lower is the harmonic degree l , the deeper is located the turning point of the mode (Fig. 5). Radial acoustic modes with $l = 0$ penetrate to the centre, while the modes of highest harmonic degree observed in the Sun ($l \simeq 1000$) are trapped in the outer 0.2% of the solar radius.

Figure 6 shows eigenfunctions for a selection of p modes with different degree: with increasing degree the p modes become confined closer and closer to the surface.

4 Helioseismic investigations

The frequencies of the solar oscillations depend on the structure of the equilibrium model, predominantly on the local adiabatic speed of sound and in addition on the variation of the density and of the adiabatic gradient in the Sun.

Moreover, the oscillation frequencies have several advantages over all the other solar observables: they can be observed with great accuracy and different modes probe the characteristics of different layers in the interior of the Sun. Thus, accurate observations of the acoustic frequencies, available today from a variety of helioseismology experiments on Earth and in space, can be used to probe the characteristics and the details of the interior of the Sun.

The goal of the helioseismology is, in fact, to infer the internal properties of the Sun and to understand the physical mechanisms which govern the behaviour of our star. This can be pursued by two different complementary strategies. The first is the forward approach which consists in comparing the observed data with the theoretical frequencies computed for a solar model, following the analysis explained in the previous sections. The second is based on the use of

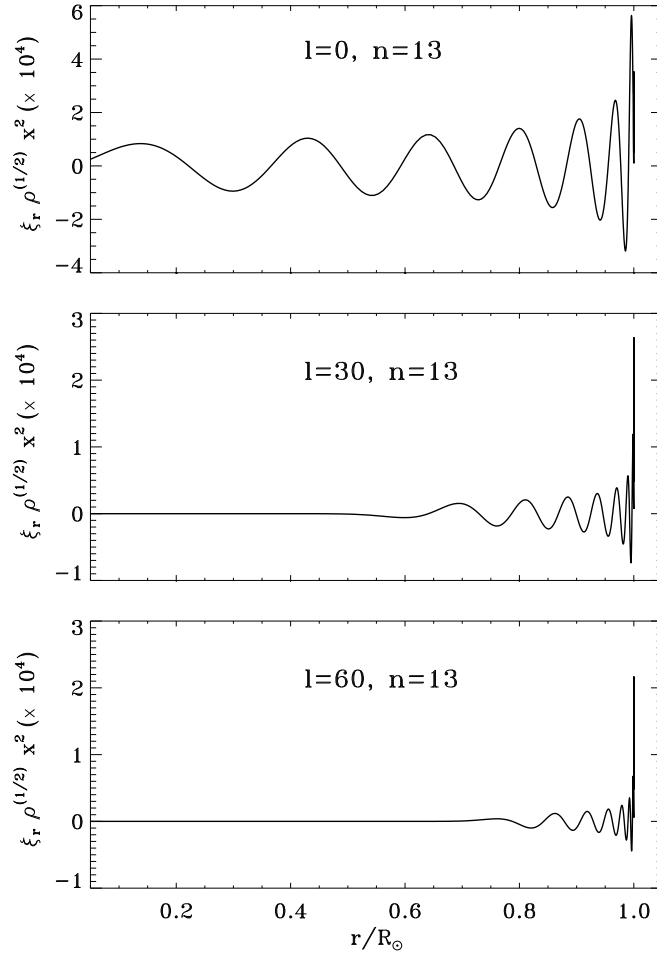


Fig. 6. Eigenfunction for p modes with different harmonic degree as function of the fractional radius $x = r/R_\odot$. Here, the oscillation behaviour is enhanced, by scaling the eigenfunctions with the square root of the density and the squared fractional radius

the observed data to deduce the internal structure and rotation of the Sun by means of data inversion. The inverse approach and its results will be extensively discussed in the next sections.

It appears clear that all the helioseismic investigations require the use of a solar model resulting from evolution of the structure equations from its formation to the present age. The computed models depend on assumptions about the physical properties of matter in stars, in particular the equation of state, the opacity and the rates of nuclear reactions.

It is also necessary that the models agree with the known non-seismic properties of the Sun: the photospheric radius $R_\odot = (6.9699 \pm 0.07) \times 10^{10} \text{ cm}$ [1],

the observed luminosity $L_{\odot} = (3.846 \pm 0.005) \times 10^{33} \text{ erg s}^{-1}$ [94], the mass $M_{\odot} = (1.989 \pm 0.0004) \times 10^{33} g$ as obtained from the study of planetary motion, the composition of the photosphere as inferred from meteoritic abundances and spectroscopic measurements $Z/X = 0.0245 \pm 0.0015$ [50], and finally the age $(4.6 \pm 0.004) \text{ Gy}$. Furthermore the computation involve some additional hypothesis and the use of an appropriate theory (e.g. mixing-length) for the treatment of the convection, to simplify the theoretical descriptions.

Here we will show results obtained by using two reference models – Model S – by Christensen–Dalsgaard et al. [18], which use respectively the OPAL [80] equation of state, and the MHD [67] equation of state. The MHD equation of state, based on the ‘chemical’ picture of the plasma, takes into account the effect of excited levels of atoms and ions on the properties of plasma and it also considers a lowest-order Coulomb coupling term through the Debye–Hückel approximation. The OPAL equation of state, in contrast, is based on a ‘physical’ description, in which nuclei and electrons (free or bound) are the only fundamental constituents of the thermodynamic ensemble.

It is important to point out that much of the uncertainty in a solar model rely on the physics which describe the surface, since there are substantial difficulties in modelling convective motions and the thermodynamic properties of this region as well as in the treatment of non-adiabatic effects on the oscillations. In most cases, in fact, the frequencies are calculated in the adiabatic approximation, which is certainly inadequate in the near-surface region.

We will limit here the considerations on the solar modelling, since this is not subject of the present review. General presentations and more detailed theory about computation of standard solar models are described in a number of standard texts, e.g. [87], [21], [24], [53].

4.1 Forward analysis

A direct way to test a solar model is to consider differences between observed frequencies and those calculated for the theoretical model. The aim of this kind of investigation is to correct the physics on which is based the solar model in such a way to reduce the discrepancies. Among several models, then, we should adopt the one which best fits the observed data.

Historically, one of the main successes of this approach was the spectacular overall agreement of the theoretical $k_h - \omega$ diagram, produced by a standard model, with the observed one, showed in the 1988 by Libbrecht [64].

Today we have the possibility to handle more accurate helioseismic observations. Here, we discuss the results produced by considering helioseismic data [75] obtained in 1996 by the MDI instrument on board the SOHO satellite [82].

Figure 7 shows the relative differences between the observed frequencies and those calculated by using Model S by Christensen–Dalsgaard et al. [18] as our reference model and it employs the OPAL [80] equation of state. The differences between the observed and calculated eigenfrequencies at low degree are very small and vary slowly with the frequency. However, at high degree the differences appear to depend on l and to increase with the frequency.

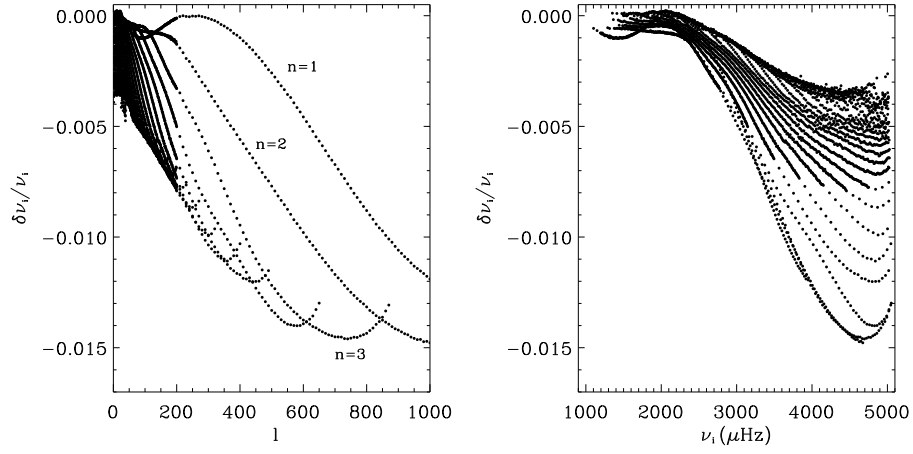


Fig. 7. Relative differences between the observed frequencies [75] obtained by MDI instrument on SOHO satellite and the theoretical frequencies computed on the reference model, as function of the degree (panel on the left) and of the frequency (panel on the right)

The frequency dependence results in part from uncertainties in the mode physics, but also from the real differences between the Sun and its reference model.

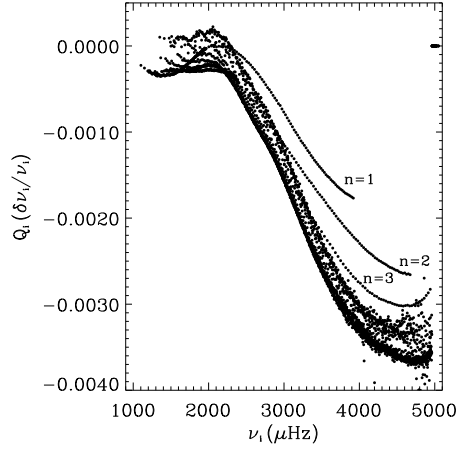


Fig. 8. Relative differences between the observed frequencies [75] and the theoretical ones (like in Fig. 7) scaled by the inertia of the mode and plotted as function of frequency

The l -dependence is mainly associated with the variation of the mode inertia, since modes with higher l penetrate less deeply and hence have a smaller inertia. Thus, high-degree modes are affected more strongly by the near-surface uncertainties [2] and [49]. The l -dependence can be isolated in part by considering frequency differences scaled by the inertia of the modes or more conveniently scaled by Q_i that is the inertia of the mode $i = (n, l)$, normalized by the inertia of a radial mode of the same frequency (see Fig. 8). The result is that the major inconsistencies, which appear at high frequency, derive from the modelling of the surface layers, indicating that the physics applied there, is inadequate for describing the relevant phenomena.

4.2 Solar seismic radius

The radius of the Sun can be simply determined from measurement of its distance and of the angular diameter of the visible disk. But, in practice it is not an easy task to distinguish the observed radius from the photospheric radius, defined as being the depth where the temperature equals the effective temperature.

The measurements of the photospheric radius obtained during the past from several groups using different instruments have provided results, which appear fairly consistent with the standard value, quoted by Allen [1].

Only in the 1997, Schou et al. [85] succeed for the first time, in obtaining an helioseismic determination of the solar radius by using high-precision measurements of oscillation frequencies of the f modes of the Sun, obtained from the MDI experiment on board the SOHO spacecraft. They determined that the seismic radius is about 300 km smaller than the model radius. A similar conclusion was reached by Antia [3] on the basis of analysis of data from the GONG network.

The helioseismic investigation of the solar radius is based on the principle that the frequencies of the f modes of intermediate angular degree depend primarily on the gravity and on the variation of density in the region below the surface, where the modes propagate. From the asymptotic dispersion relation (30), one can easily deduce that $\omega \propto R_\odot^{-3/2}$. Therefore, by applying a variational principle, we can obtain a relation between f-mode frequencies, $\omega_{l,0} = 2\pi\nu_{l,0}$, and the correction ΔR that has to be imposed to the photospheric radius R_\odot assumed for the standard solar model:

$$\frac{\Delta R}{R_\odot} = -\frac{2}{3} \left\langle \frac{\Delta\nu_{l,0}}{\nu_{l,0}} \right\rangle, \quad (34)$$

where $\langle \rangle$ denotes the average weighted by the inverse square of the measurement errors.

Dziembowski et al. [37], by analyzing a long time-series of MDI f-mode frequencies, inferred temporal variation of the solar radius, with the aim of determining a possible solar cycle dependence. Their first results (Fig. 9), covering the period from May 1996 to April 1997, show that the maximal relative variation of the solar radius during the observed period was about $\Delta R/R_\odot = 6 \times 10^{-6}$, which corresponds to approximately $\Delta R = 4$ km. Recently, Dziembowski et al. [38] analyzing a larger set of data spanning a period from mid 1996 to mid 1999, have

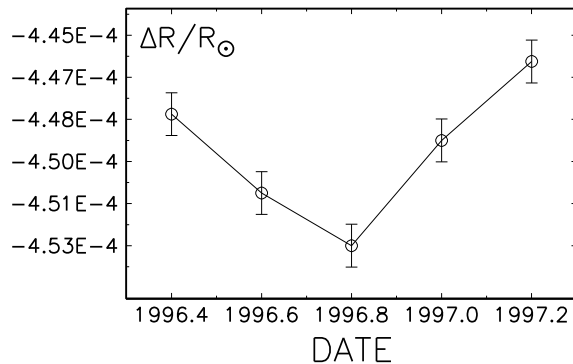


Fig. 9. Relative differences in radius of the Sun inferred from the f-mode frequencies and the standard solar model as in [37]

found that the systematic trend of $\Delta R/R_{\odot}$ is not correlated with the magnetic activity.

However, Brown & Christensen-Dalsgaard [11], by combining photoelectric measurements with models of the solar limb-darkening function, determined a photospheric radius of 695.508 ± 0.026 *Mm*. This value appears even smaller than the helioseismic one and the reason for this discrepancy is still unknown.

It is clear that the problem that remains to be clarified is the connection between the seismic radius determined from helioseismic measurements and the definitions of solar radius as obtained from the other methods.

5 Helioseismic inversion

The inverse problem, always associated with the forward approach, involves estimating some functions to describe the physical properties of the Sun, by solving integral equations which appear expressed in terms of the experimental data. Inversion techniques are well known and applied with success in several branches of the physics from geophysics to the radiation theory, as reported in [70], [26] and [90]. Applications to the helioseismic data have been studied extensively during the last decade and inversion methods and techniques have been reviewed and compared by several authors, e.g. [48], [27], [55], [39], [4] and [47].

The observed data are related to the physics of the solar structure, in a very complicated way, and the main difficulty arises from the fact that the helioseismic inversion is an ill-posed problem:

- For each set of data, there exists an infinite number of solutions
- The solution is not unique
- The solution does not depend continuously on the data.

In fact, the observed frequencies constitute a finite set of data and the errors in the observations prevent the solution from being determined with certainty. Thus, an appropriate choice of a suitable technique of inversion is the first important strategy to adopt during a helioseismic inverse analysis.

The first attempts at inversion used analytical methods to solve integral equations obtained in first approximation by applying the asymptotic dispersion relation of solar frequencies, the so-called Duvall law [34]. This inversion method is considered however not very accurate, since the Duvall law represents a rough approximation for the low degree modes which are the more appropriate to study the Sun's core. For this reason, here we will consider only numerical techniques of inversion.

5.1 Inversion Techniques

Since most of the fundamental aspects of inversion do not depend on the dimensions of the space in which the problem is posed, for simplicity here we consider the general case of the linear one-dimensional inversion problem, in which the measured data d_i are functionals of a single function, $f(r)$, of the distance to the centre r :

$$d_i = \int_0^{R_\odot} \mathcal{K}^i(r) f(r) dr + \varepsilon_i \quad i = 1, \dots, M \quad (35)$$

where R_\odot is the radius of the Sun. The properties of the inversion depend both on the mode selection $i \equiv (n, l)$ and on the observational errors ε_i , which characterize the mode set ($i = 1, \dots, M$) to be inverted.

The observational errors ε_i in the data, are assumed to be independent and Gaussian-distributed with zero mean and variances σ_i^2 . Given a set of data and errors, the problem is to determine $f(r)$ by solving the Eq. (35), where $\mathcal{K}^i(r)$, the kernels of the integral, are known functions which depend on the quantities of the reference model and its eigenfunctions.

There are two important classes of methods of obtaining estimates of $f(r)$: optimally localized averaging method based on the original idea of Backus & Gilbert [5], [6] and regularized least-squares fitting method due to Phillips [71] and Tikhonov [91]. Both methods give linear estimates of the function $f(r)$ and give results in general agreement, as it was demonstrated by Christensen-Dalsgaard et al. [20] and by Sekii [88].

Optimally localized averaging (OLA) The localized averaging kernel method allows us to solve Eq. (35) by estimating a localized weighted average of the unknown generic quantity $f(r)$ at selected target radii r_0 's by means of a linear combination of all the data d_i :

$$\bar{f}(r_0) = \sum_{i=1}^M \alpha_i(r_0) d_i = \sum_{i=1}^M \alpha_i(r_0) \int_0^{R_\odot} \mathcal{K}^i(r) f(r) dr, \quad (36)$$

where $\alpha_i(r_0)$ are the inversion coefficients to be found and

$$K(r_0, r) = \sum_{i=1}^M \alpha_i(r_0) \mathcal{K}^i(r) \quad (37)$$

are the so called 'averaging kernels'.

Because of the ill-conditioned nature of the inversion problem, it is necessary to introduce a regularization procedure. By varying a trade-off parameter θ , we look for the coefficients $\alpha_i(r_0)$ which minimize the propagation of the errors and the spread of the kernel:

$$\int_0^{R_\odot} J(r_0, r) K(r_0, r)^2 dr + \tan \theta \sum_{i=1}^M \sigma_i^2 \alpha_i^2(r_0) , \quad (38)$$

assuming that

$$\int_0^{R_\odot} K(r_0, r) dr = 1 . \quad (39)$$

$J(r_0, r)$ is a weight function that is small near r_0 and large elsewhere, assumed to be:

$$J(r_0, r) = (r - r_0)^2 . \quad (40)$$

From Eq. (38) we obtain the expression for the inversion coefficients:

$$\alpha_i(r_0) = \sum_{j=1}^M [S_{ij}(r_0) + \tan \theta E_{ij}]^{-1} \int_0^{R_\odot} \mathcal{K}^j(r) dr , \quad (41)$$

where

$$S_{ij}(r_0) = \int_0^{R_\odot} (r - r_0)^2 [\mathcal{K}^i(r) \mathcal{K}^j(r)] dr , \quad (42)$$

and the diagonal covariance matrix of the errors has elements:

$$E_{ij} = \begin{cases} \sigma_i^2 \alpha_i^2(r_0) & \text{for } i = j \\ 0 & \text{for } i \neq j \end{cases} \quad (43)$$

By lowering the trade-off parameter it is possible to obtain more localized averaging kernels closer to the nominal point $r = r_0$, but this decreases the accuracy with which the solution is determined, since the importance of the errors increases. Thus, we should choose, among all the possible solutions, an optimal compromise between localization and accuracy of the solution.

The Eq. (41) is equivalent to solve the following set of linear equations:

$$A(r_0) \boldsymbol{\alpha}(r_0) = \mathbf{b} , \quad (44)$$

where $\boldsymbol{\alpha}(r_0)$ represents the vector for each target radius, whose M elements are the coefficients $\alpha_i(r_0)$; \mathbf{b} is the vector which contains the Lagrangian multipliers; $A(r_0)$ is the $M \times M$ symmetric matrix, whose elements for each r_0 are $a_{ij} =$

$S_{ij}(r_0) + \tan \theta E_{ij}$. Therefore, the OLA method is very much demanding on computational resource, since it requires the inversion of N matrixes of order M to determine the solution at N radial points.

The errors of the solutions are the standard deviations calculated in the following way:

$$\delta \bar{f}(r_0) = \left[\sum_{i=1}^M \alpha_i^2(r_0) \sigma_i^2 \right]^{1/2}, \quad (45)$$

while the radial spatial resolution is assumed to be the half-width at half-maximum of the resolving kernels.

The same method can be applied in the variant form described by Pijpers and Thompson in [73] and [74], known as SOLA method (Subtractive Optimally Localized Averaging), making attempts to fit the averaging kernel to a target function, usually a Gaussian function $G(r_0, r)$, of appropriate width and centered at the target radiulos:

$$K(r_0, r) \simeq G(r_0, r) \simeq \delta(r_0, r). \quad (46)$$

In this case, the trade-off parameter is rescaled at each target location to keep constant the width of the averaging kernels and to obtain more localized resolving kernels closer to the nominal concentration point. Therefore, the coefficients are determined by minimizing the following:

$$\int_0^{R_\odot} \left[\sum_{i=1}^M \alpha_i(r_0) \mathcal{K}^i(r) - G(r_0, r) \right]^2 dr + \tan \theta \sum_{i=1}^M \sigma_i^2 \alpha_i^2(r_0), \quad (47)$$

so that

$$\alpha_i(r_0) = \sum_{j=1}^M (U_{ij} + \tan \theta E_{ij})^{-1} \int_0^{R_\odot} \mathcal{K}^i(r) G(r_0, r) dr, \quad (48)$$

where

$$U_{ij} = \int_0^{R_\odot} [\mathcal{K}^i(r) \mathcal{K}^j(r)] dr. \quad (49)$$

This inversion problem appears equivalent to solve the following set of linear equations:

$$\mathbf{W} \boldsymbol{\alpha}(r_0) = \mathbf{g}(r_0), \quad (50)$$

where \mathbf{W} is a matrix whose elements are $w_{ij} = U_{ij} + \tan \theta E_{ij}$, and hence does not depend on r_0 ; $\mathbf{g}(r_0)$ is the cross-correlation vector of the kernels with the target function $G(r_0, r)$. Thus, the solutions are obtained by inverting the matrix \mathbf{W} only one time, such that the computational efforts is therefore reduced substantially.

Regularized Least-Squares Fitting (RLS) This method allows to find a solution that is expressed as a linear combination of a chosen set of base functions ϕ_j with $j = (1, \dots, N)$:

$$\bar{f}(r) = \sum_{j=1}^N f_j \phi_j(r) , \quad (51)$$

where f_j are constants to be determined.

We can choose the base functions, for example, being piecewise constant functions on a dissection r_j of the interval $[0, R_\odot]$:

$$\phi_j(r) = \begin{cases} 1 & r_{j-1} < r < r_j \\ 0 & \text{elsewhere} \end{cases} \quad (52)$$

so that $\bar{f}(r) = f_j$ on the interval $[r_{j-1}, r_j]$. Other common alternatives are to choose $\phi_j(r)$ as a continuous set of piecewise linear functions or as a set of splines.

The parameters f_j are determined by a least-squares fit to the data. However, this procedure needs a regularization procedure to obtain a smooth solution. So, basically we can determine the constants by minimizing:

$$\sum_{i=1}^M \frac{1}{\sigma_i^2} \left[d_i - \int_0^{R_\odot} \mathcal{K}^i(r) \bar{f}(r) dr \right]^2 + \mu \int_0^{R_\odot} [\mathcal{F} \bar{f}(r)]^2 dr , \quad (53)$$

where μ is a trade-off parameter between resolution and error and \mathcal{F} is a differential operator so that $\mathcal{F} \bar{f}(r)$ is a suitable weight function that determines the relative importance of smoothing in different regions.

The minimization of the (53) leads to a set of linear equations which permits to determine f_j and hence the solutions.

6 Inversions for the solar structure

6.1 The variational principle

The numerical inversion of data to determine the solar structure is based on the use of the variational principle of Chandrasekhar [12]. Thus, the eigenfrequencies can be determined by solving an eigenvalue problem, whose expression can be obtained directly from the basic equations governing linear adiabatic oscillations Eqs. (9a)–(9d):

$$\omega^2 \delta \mathbf{r} = \mathcal{F}(\delta \mathbf{r}) , \quad (54)$$

where ω^2 are the eigenvalues, \mathcal{F} is a linear operator on the eigenfunctions $\delta \mathbf{r}$.

Although the frequencies of solar oscillations can be known from observations, the eigenfunctions cannot be determined experimentally, so Eq. (54) define a nonlinear integral equation.

However, Eq. (54) can be linearized around a known reference model, under the assumption of hydrostatic equilibrium. This procedure, whose details can be found, e.g., in [93], provides a linear integral equation that can be used in an inverse procedure to determine the corrections which have to be imposed to the reference model in order to obtain the observed oscillation frequencies $\omega_i = 2\pi\nu_i$.

6.2 The surface term

Non-adiabatic effects and other errors in modelling the surface layers, that can give rise to frequency shifts, as it was explained in Section 4.1, have to be taken into account by including an arbitrary function of frequency $F_{\text{surf}}(\nu)$ in the variational formulation, as suggested by Dziembowski et al. in [40].

The function $F_{\text{surf}}(\nu)$ must be determined as part of the analysis of the frequency differences. It should resemble, in practise, the differences $Q_i \delta \nu_i / \nu_i$ plotted in Fig. (8). As $F_{\text{surf}}(\nu)$ is assumed to be a slowly varying function of frequency, it can be expressed as expansion of Legendre polynomials $P_\lambda(\nu)$, usually of low degree λ .

In the inversion procedures it is common use to suppress the surface term [27]. This is done by constraining the inversion coefficients to satisfy:

$$\sum_{i=1}^M \alpha_i P_\lambda(\nu_i) Q_i^{-1} = 0 \quad \lambda = 0, 1 \dots \Lambda. \quad (55)$$

The maximum value of the polynomial degree, Λ , used in the expansion is a free parameter of the inversion procedure. In practice, we should consider an appropriate value of Λ for any given data set.

6.3 Inversion for sound-speed and density

It follows, from the preceding discussion, that the differences in, for example, sound speed c and density ρ between the structure of the Sun and the reference model ($\delta c^2/c^2$, $\delta \rho/\rho$) can be expressed by the following integral equation [40]:

$$\frac{\delta \nu_i}{\nu_i} = \int_0^{R_\odot} K_{c^2}^i(r) \frac{\delta c^2}{c^2}(r) dr + \int_0^{R_\odot} K_\rho^i(r) \frac{\delta \rho}{\rho}(r) dr + \frac{F_{\text{surf}}(\nu)}{Q_i} + \varepsilon_i, \quad (56)$$

where $K_{c^2, \rho}^i$ and K_{ρ, c^2}^i are the kernels. The term Q_i has been already introduced in Section 4.1.

Equation (56) forms the basis for the linearized structure inversion. Unlike the case considered in Section 5.1, this linearized inverse problem involves three unknown functions: $\delta c^2/c^2$, $\delta \rho/\rho$ and $F_{\text{surf}}(\nu)$. However, the number of the unknown functions can be reduced to one by adapting the method of the optimally localized averages.

The principle of the inversion, by generalizing the SOLA technique (see Eq. 47), is to form a linear combinations of $\delta \nu_i / \nu_i$ with coefficients $\alpha_i(r_0)$ chosen to minimize:

$$\int_0^{R_\odot} [\mathcal{K}(r_0, r) - \mathcal{G}(r_0, r)]^2 dr + \beta \int_0^{R_\odot} \mathcal{C}^2(r_0, r) f(r) dr + \mu \sum_{i=1}^M \alpha_i^2(r_0) \sigma_i^2, \quad (57)$$

where

$$\mathcal{K}(r_0, r) = \sum_{i=1}^M \alpha_i(r_0) K_{c^2, \rho}^i(r) \quad (58)$$

are the *averaging kernels*, while

$$\mathcal{C}(r_0, r) = \sum_{i=1}^M \alpha_i(r_0) K_{\rho, c^2}^i(r) \quad (59)$$

are the *cross-term kernels*. The parameter β control the balance between the contribution from $\delta\rho/\rho$ on $\delta c^2/c^2$; μ is the trade-off parameter, determining the balance between the demands of well-localized kernels and a small error in the solution; $f(r)$ is a suitably increasing function of radius aimed at suppressing the surface structure in the cross-term kernel, e.g. we can use $f(r) = (1 + r/R)^4$.

Thus, if our goal is to infer the speed of the sound, the coefficients $\alpha_i(r_0)$ should be chosen such to suppress the contribution from the cross term, to localize the averaging kernel near $r = r_0$, to suppress the surface term assuming the (55), while limiting the error in the solution, by the use of the two parameters β and μ .

Inversion results The first significant results concerning the application of the inversion technique to the Sun were obtained in 1985 by Christensen–Dalsgaard et al. [19], who produced the sound speed profile in the interior of the Sun and who first determined the location of the base of the convection zone. Since then, several efforts have been done for inverting data in order to test the correctness of the standard models in view of the improvements accomplished in the description of the relevant physics. A significant progress, in particular, has been achieved with the inclusion of diffusion of helium and heavy elements at the base of the convective zone [9].

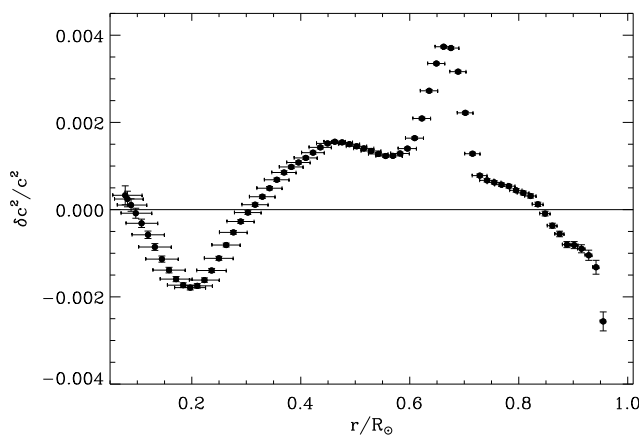


Fig. 10. The relative squared sound-speed difference between the Sun and the standard solar model [18] as obtained by inversion of MDI/SOHO data [83]

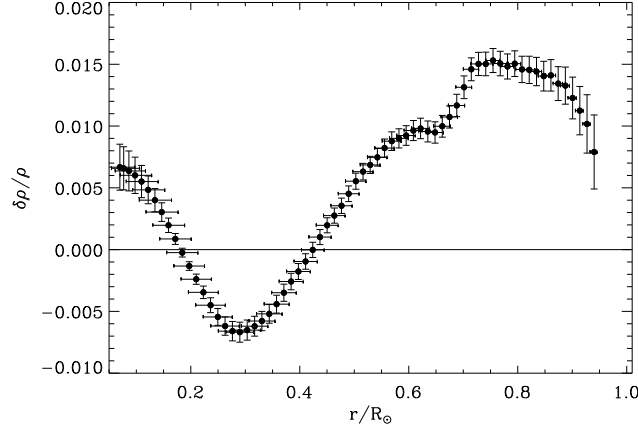


Fig. 11. The relative squared density difference between the Sun and standard solar model [18] as obtained by inversion of MDI/SOHO data [83]

The resulting profiles for the speed of the sound and for the density, which are shown here, have been obtained by inversions of high quality helioseismic data obtained during 1998 by Schou [83], from SOI-MDI [82] instrument on SOHO satellite. This set includes only modes with harmonic degree $l \leq 100$.

The Model S [18] which employs the OPAL [80] equation of state is used here as reference model.

Figures 10 and 11 show the behaviour of the relative squared sound-speed and density differences between the Sun and the standard solar model as function of the fractional radius. The vertical error bars correspond to the standard deviations based on the errors in the mode sets, calculated by Eq. (45), whereas the horizontal bars give a measure of the localization of the solution. The results indicate the substantial correctness of the standard solar models. In fact, it is clear that deviations are extremely small, except below the base of the convection zone ($0.71 R_\odot$) where the theory fails to correctly describe the turbulent convection.

The structure of the core, however, is still quite uncertain since the few modes with lowest harmonic degree that are able to penetrate towards the centre, sample the core for a relative short time because of the large sound speeds there.

6.4 Inversion for equation of state and the solar helium abundance

The equation of state can be investigated through the first adiabatic exponent Γ_1 , the partial logarithmic derivative of pressure with respect to density at constant specific entropy, already defined in Eq. (6).

The solar plasma is almost an ideal gas, and the first adiabatic exponent is therefore close to $5/3$ in most of the interior. It deviates from this value in the

zones of hydrogen and helium ionization, near the surface. Therefore, inversions of helioseismic data can be used, in particular, to study the equation of state and to probe the helium abundance in the solar envelope, as it was proved e.g. in [46], [56], [42], [8].

An integral equation analogous to Eq. (56) can be derived to determine the behaviour of $(\delta\Gamma_1/\Gamma_1)_{\text{int}}$ the relative intrinsic difference in Γ_1 , at constant pressure p , density ϱ and composition, between the equation of state of the Sun and the one of the reference model, as in [8].

The kernels for (c^2, ϱ) which appear in Eq. (56) can be converted to kernels for the set (Γ_1, u, Y) , where $u \equiv p/\varrho$ and Y the helium abundance. After the conversion, Eq. (56) can be written as

$$\begin{aligned} \frac{\delta\nu_i}{\nu_i} = & \int_0^{R_\odot} K_{c^2, \varrho}^i \left(\frac{\delta\Gamma_1}{\Gamma_1} \right)_{\text{int}} dr + \int_0^{R_\odot} K_{u, Y}^i \frac{\delta u}{u} dr \\ & + \int_0^{R_\odot} K_{Y, u}^i \delta Y dr + \frac{F_{\text{surf}}(\nu)}{Q_i} + \varepsilon_i, \end{aligned} \quad (60)$$

where $(\delta\Gamma_1/\Gamma_1)_{\text{int}}$ is the difference in Γ_1 that results from the differences in the equation of state alone, but not from the resulting change in solar structure. The term δY denotes the difference of the helium abundance in the convective zone between the Sun and the model.

According to the the OLA technique of inversion (Section 5.1), the coefficients are found by minimizing:

$$\begin{aligned} & \int_0^{R_\odot} \mathcal{K}^2(r_0, r) J(r_0, r) dr + \beta_1 \int_0^{R_\odot} \left(\sum_{i=1}^M \alpha_i(r_0) K_{u, Y}^i \right)^2 f(r) dr \\ & + \beta_2 \int_0^{R_\odot} \left(\sum_{i=1}^M \alpha_i(r_0) K_{Y, u}^i \right)^2 f(r) dr + \mu \sum_{i=1}^M \alpha_i^2(r_0) \sigma_i^2. \end{aligned} \quad (61)$$

The parameters β_1 and β_2 control the contributions of $\delta u/u$ and δY , respectively, and μ is a trade-off parameter which controls the effect of data noise. As in Eq. (38) $J(r_0, r)$ is a weight function; $f(r)$ is included to suppress surface structure in the first and second cross-term kernels, like in Eq. (57).

Figure 12 from Di Mauro & Christensen-Dalsgaard [30], shows the resulting intrinsic differences in Γ_1 between the Sun and the two available equations of state (OPAL and MHD), as obtained by inversion of the data set by Schou [83], which includes only modes with low and intermediate harmonic degree ($l \leq 100$).

As already shown by Basu & Christensen-Dalsgaard [8], by using only low and intermediate-degree modes it is difficult to judge the significance of the differences between the two equations of state. Nevertheless, Fig. 12 confirms previous findings by Elliott & Kosovichev [43] that Γ_1 deviate from 5/3 in the central core, probably due to relativistic effects.

The results shown in Fig. 13, as found in Di Mauro & Christensen-Dalsgaard [31], have been carried out by inversion of preliminary helioseismic data by

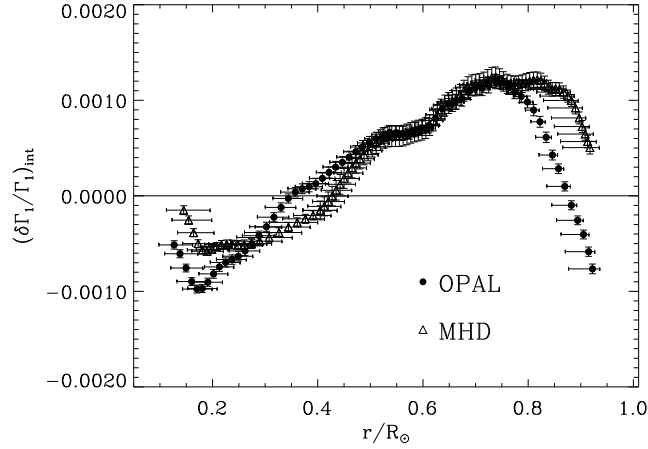


Fig. 12. The intrinsic difference in the adiabatic exponent Γ_1 between the Sun and the OPAL [80] equation of state (filled circle) and the Sun and the MHD equation of state [18] (open triangles) obtained by inversion of a set of data by Schou [83], which does not include high-degree modes

Rhodes et al. [75], which include high-degree modes ($l < 1000$), obtained in 1996 by the MDI instrument on board the SOHO satellite. The set is made up of a very large number of data (7480 modes), which makes the computations slow and very demanding in terms of computer memory. The precise high-degree modes are able to determine variations very near the solar surface, through the He II ionization zone and also part of the He I ionization zone, while by using only low and intermediate-degree modes (Fig. 12), we cannot determine solutions above $r \simeq 0.96R_\odot$.

From Fig. 13 we can affirm that, as noticed by Basu et al. [10], the OPAL equation of state is able to describe better the plasma conditions in the interior of the Sun below $0.97R_\odot$. In the upper layers above $0.97R_\odot$, the results indicate a large discrepancy between the models and the observed Sun, even considering higher-order asymptotic terms in F_{surf} . Here, the use of very high degree modes reveals that the differences between the two equations of state are very small. This is in contrast to earlier results by Basu et al. [10], which found evidence, by inverting a set of data with no highest degree modes, that MHD models give a more accurate description of the very upper layers than the OPAL models.

The helium abundance in the solar envelope It is well known that spectroscopic measurements of the photospheric abundance of helium (Y_\odot) in the Sun are very uncertain and, before the advent of helioseismology, the only accurate method to quantify Y_\odot was based on a calibration of solar models, in which

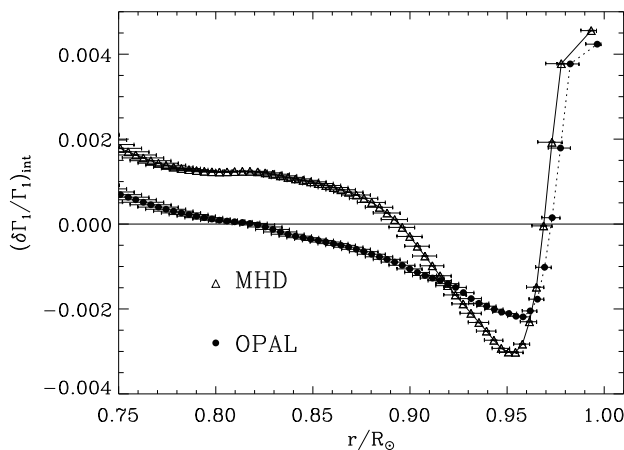


Fig. 13. The intrinsic difference in the adiabatic exponent Γ_1 between the Sun and the OPAL [80] equation of state (filled circle) and the Sun and the MHD [67] equation of state (open triangles) obtained by inversion of a set of data by Rhodes et al. [75], which includes high-degree modes

the helium abundance has to be adjusted to match the observed solar luminosity. The value of helium abundance calibrated with this method is typically about 0.27.

In the 1984, Gough [46] noted that the strong sensitivity of acoustic modes to the variation of the adiabatic exponent in the HeII ionization zone could allow also a seismic determination of the helium abundance in the outer layers of the Sun. Thus, equations like (61), may be inverted to determine δY , the difference between the helium abundance of the Sun and that of the solar model in the helium ionization zones [40]. Since the convection zone is fully mixed, this provides a measure of the value of the helium abundance in the solar envelope. It is also important to point out that the determination of the solar helium abundance, inferred from the inversion of data, is sensitive to the equation of state employed in the reference model.

The first seismic measures of Y_\odot obtained by Christensen-Dalsgaard et al. [18] reported values between 0.24 and 0.25, that were significantly less than the abundance estimated by the calibration on the standard solar model. Dziembowski et al. [41] pointed out that the difference was in rough agreement with that expected by the effect of gravitational settling of helium and heavy elements, as calculated by Cox et al. [25]. So, today settling is contained in all the most accurate standard solar models.

Recently, Di Mauro & Christensen-Dalsgaard [31] have used Eq. (61) to determine δY , by inverting a set of data with high degree acoustic frequencies [75]. By using the MHD equation of state, they obtained a value of 0.2426 ± 0.0005 ,

consistent with the earlier results by Kosovichev [57] and Richard et al. [76], which employed a similar variational technique. By considering the OPAL equation of state they obtained a value of 0.2648 ± 0.0004 , which is strikingly higher than previous values quoted in the literature ($\simeq 0.242 - 0.25$) by Basu & Antia [7], Kosovichev [57], Richard et al. [77] and Basu et al. [10].

The rather high value obtained for the helium abundance based on the OPAL model may be due to the use of a set with very high degree modes. The determination of observational frequencies for high-degree modes still suffers from substantial difficulties, related to the merging of power into ridges and the proper treatment of the leakage matrix (e.g. [83]) and this could cause systematic errors in the frequencies.

7 Dynamics of the Sun

7.1 Fine structure in the acoustic spectrum of oscillations

So far, we have considered only oscillations of a spherically symmetric structure, but it is well known and easily observed at the photosphere that the Sun is a slowly rotating star.

The rotation breaks the spherical symmetry of the solar structure and splits the frequency of each oscillation mode of harmonic degree l into $2l + 1$ components. Multiplets with a fixed n and l are said to exhibit a frequency “splitting” defined by:

$$\Delta\omega_{n,l,m} = \omega(n, l, m) - \omega(n, l, 0) , \quad (62)$$

somewhat analogous to the Zeeman effect on the degenerate energy levels of an atom.

The determination of the splittings is often very difficult, so generally, the observations have not been applied in terms of individual mode frequencies, but rather it is customary to represent the frequency splittings by polynomial expansion in terms of the so called a -coefficients, as explained in [84]:

$$\omega(n, l, m) = \omega(n, l, 0) + 2\pi \sum_{j=0}^{j_{max}} a_j(n, l) \mathcal{P}_j^{(l)}(m), \quad (63)$$

where $\mathcal{P}_j^{(l)}(m)$ are orthogonal polynomials that can be chosen, for example, like Ritzwoller and Lavelly in [78]. Because of the symmetry properties of the splittings, the solar rotation is described only by the odd coefficients a_j , while the even coefficients are a measure of the Sun’s asphericity.

7.2 Inversion for solar rotation

To study the dynamics of the Sun we need to reconsider the derivation of the basic oscillation equations (19a)–(19c) by including the effect of a velocity field. We assume that the rotation is sufficiently slow that the centrifugal force and

other effects of second and higher order can be neglected. This treatment allows to define a new expression which relates eigenfrequencies with eigenfunction and physical quantities, like the Eq. (54). By applying standard perturbation theory to the eigenfrequencies, it can be shown that the rotational splittings are related to the rotation rate $\Omega(r, \theta)$ inside the Sun by:

$$\Delta\omega_{n,l,m} = \int_0^{R_\odot} \int_0^\pi \mathcal{K}^{n,l,m}(r) \Omega(r, \theta) r dr d\theta \quad (64)$$

where θ is the colatitude and $\mathcal{K}^{n,l,m}(r)$ are the mode kernel functions. The dependence of the splittings on angular velocity can be used in a 2-dimensional inverse problem to probe the dynamics of the Sun.

The 2-dimensional inverse problem can be simplified by considering that the expansion of the splittings in polynomials given in the Eq. (63) corresponds to an expansion of $\Omega(r, \theta)$ such that:

$$\Omega(r, \mu) = \sum_{j=0}^{j_{max}} \tilde{\Omega}_{2j+1}(r) \frac{dP_{2j+1}(\mu)}{d\mu} \quad (65)$$

where $P_{2j+1}(\mu)$ are the Legendre polynomials with $\mu = \cos \theta$. So, the a -coefficients are related to the expansion functions $\tilde{\Omega}_{2j+1}(r)$ by:

$$2\pi a_{2j+1}(n, l) = \int_0^{R_\odot} \mathcal{K}_j^{n,l}(r) \tilde{\Omega}_{2j+1}(r) dr \quad (66)$$

in which the kernels are calculated according to the expressions given in [33].

Equation (66) constitutes the basis for the 1.5-dimensional inversion. Now, the original inverse problem Eq. (64) has been decomposed into a series of 1-dimensional independent inversions for each a -coefficient to determine the expansion functions $\tilde{\Omega}_{2j+1}(r)$, whose combination according to Eq. (65) leads to:

$$\Omega(r, \mu) = \tilde{\Omega}_1(r) + \tilde{\Omega}_3(r) \frac{dP_3(\mu)}{d\mu} + \tilde{\Omega}_5(r) \frac{dP_5(\mu)}{d\mu} + \dots \quad (67)$$

7.3 Inversion results

The variation of the Sun's angular velocity with latitude and radius shown here, has been determined by Di Mauro et al. [33] by means of a 1.5 dimension SOLA helioseismic inversion of more than 30,000 p -mode splitting coefficients. These data were obtained from the first set of uninterrupted Doppler images from SOI-MDI (on board the SOHO satellite) in 1996 [86], which yield splittings of great accuracy, never obtained in previous sets of data.

The inferred rotation rate is shown in Fig. 14 where the points indicate the angular velocity at various depths calculated at the equator, and at latitudes of 30° , 60° and 75° .

In Fig. 15 contours and red-scale indicate isorotation surfaces in a cut of the interior of the Sun. The results confirm the previous findings that the latitudinal differential rotation observed at the surface persists throughout the convection zone, while the radiative interior rotates almost rigidly at a rate of about 430 nHz . At low latitudes the angular velocity, through the largest part of the convection zone, decreases with the radius while at high latitudes increases inwards. The near-surface behaviour agrees with the observed surface rotation rate.

The tachocline, the transition layer from latitudinally-dependent rotation to nearly independent rotation [89], is of very considerable dynamical interest. Furthermore, it is thought that the global dynamo behaviour, responsible for the solar 11 years magnetic cycle, rises from strong toroidal magnetic fields generated by rotational shear in this thin region.

The tachocline appears mostly located in the radiative zone at a pretty sharp midpoint near about $r = 0.693 R_\odot$ according to Corbard et al. [22], and near $r = 0.695 R_\odot$ for Charbonneau et al. [15]. It is also a fairly thin layer, not more than $0.05 R_\odot$ at the equator. The layer seems to be wider at high latitudes, but certainly less than $0.1 R_\odot$ [32]. Charbonneau et al. [15], have recently confirmed that the width of the tachocline appears to change with the latitude, with a minimum value at the equator of $(0.0039 \pm 0.0013) R_\odot$.

Another interesting dynamical feature occurs near the poles, where unfortunately it is very difficult to localize the inversion solutions. Fig. 14 shows the

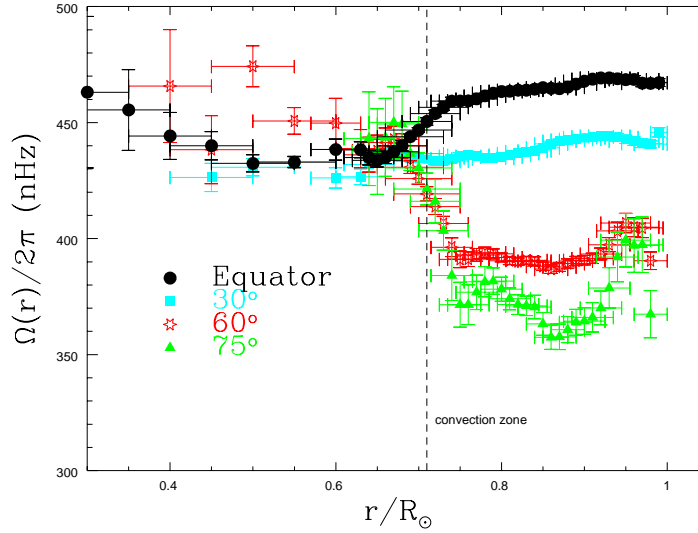


Fig. 14. Differential rotation at four latitudes as obtained by a 1.5 dimensional SOLA inversion of the SOI-MDI data. The approximate base of the convection zone is indicated by the dashed line [33]

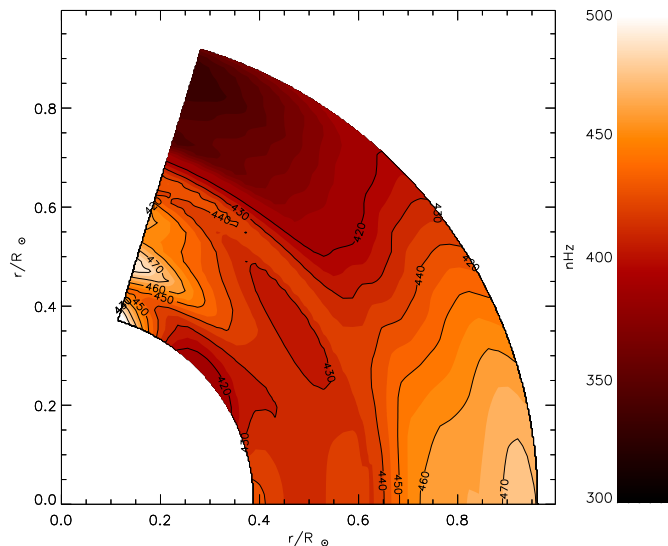


Fig. 15. Rotation rate in the Sun obtained by inversion of MDI data. Colours and contours indicate the isorotation surfaces. The white area indicates the region in the Sun where the data have no reliable determinations [33]

presence at latitude of 75° of a fairly localized region rotating faster than the surroundings [86]. It is still not clear, if this feature is somewhat related to the applied inversion technique.

Very recently, Howe et al. [51] have found evidence that the rotation rate near the base of the convective envelope shows variations with time, with a period of the order of 1.3 yr at low latitude. Such variations occur above and below the tachocline and appear more pronounced near the equator and at high latitudes.

To infer accurately the rotation in the deepest interior, it is necessary to invert a set of data which includes accurate splittings of the lowest degree modes ($l = 1 - 4$). The data sets, available for this purpose are obtained by the ground-based networks BiSON [14], IRIS [61] and GONG [45] and from the GOLF [79] instrument on SOHO. Unfortunately these sets of data are not in mutual agreement and give conflicting results of inversion in the core, as it is shown in Fig. 16, taken from Di Mauro et al. [33]. Here, the radial spatial resolution, for clarity not drawn in the figure, is fixed at $\Delta r = 0.1 R_\odot$. The independent sets of observations obtained by IRIS, GONG, GOLF lead to the conclusion that the Sun's core is in a state of rotation slightly faster than that observed at the surface in contradiction with the BiSON's data inversion which indicates a central angular velocity even slower than the surface polar angular velocity, as it was recently confirmed by Chaplin et al. [13]. Thus, the kinematics in the core remains largely uncertain, with a disagreement that might derive from the different data analysis procedures employed.

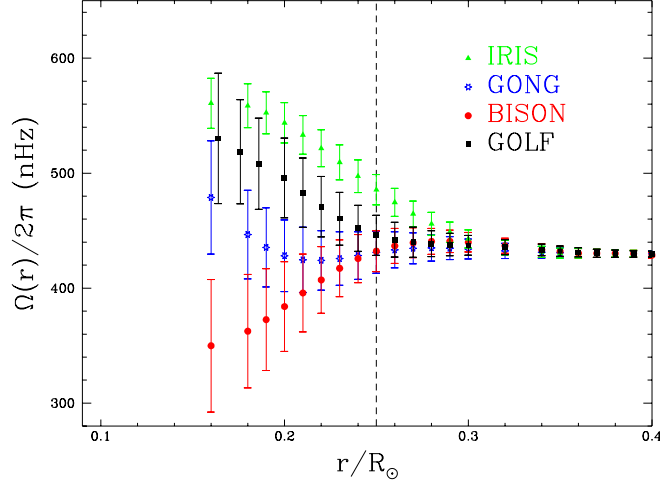


Fig. 16. Rotation of the Sun’s core as deduced by inversion of the BISON (filled circles), IRIS (filled triangles), GONG (starred symbols) and GOLF (filled squares) sets of lowest degree splittings ($l = 1 - 4$), all combined with MDI higher degree data set. The radial spatial resolution of each radial point is fixed at $\Delta r = 0.1 R_\odot$

7.4 Helioseismic determination of the solar angular momentum and quadrupole moment

The present angular momentum of the Sun \mathfrak{S} , can be deduced from the internal rotational behaviour derived from helioseismological data, by integrating the following [33]:

$$\mathfrak{S} = \int_0^{M_\odot} r^2 dM_r \int_0^1 (1 - \mu) \Omega(r, \mu) d\mu = \frac{2}{3} \int_0^{M_\odot} \tilde{\Omega}_1(r) r^2 dM_r, \quad (68)$$

where $\tilde{\Omega}_1(r)$ is determined by helioseismic inversion of the a_1 -splitting coefficient, from Eq. (66). If we assume the angular velocity behaviour shown in Fig. 14, the integration of Eq. (68) leads to $\mathfrak{S} = (1.96 \pm 0.05) \cdot 10^{48} \text{ g cm}^2 \text{ sec}^{-1}$ [33]. This value is in agreement within errors with the one obtained by Pijpers in [72].

Another quantity of particular interest is the gravitational quadrupole moment J_2 of the Sun, which can be deduced, according to Pijpers [72] by evaluating the two-dimensional integral:

$$J_2 = \int_0^{R_\odot} dr \int_{-1}^1 \mathcal{F}(r, \mu) \Omega^2(r, \mu) d\mu, \quad (69)$$

where $\mathcal{F}(r, \mu)$ is the two-dimensional kernel which depends on the physical quantities of the reference model and on some more general assumptions on the physics of the Sun.

The value of J_2 obtained by Pijpers [72] is $J_2 = (2.23 \pm 0.09) \times 10^{-7}$. This result is totally consistent with the one obtained by Paternò et al. [69] with a different approach based on both the measurement of solar oblateness and the angular velocity profile deduced by inversion of splittings.

8 Seismology of the fine structure: solar asphericities

The asymmetric part of the fine structure in the p-mode spectrum (Eq. 63) of solar oscillations varies in a systematic way through the solar cycle [58], [59], [65].

It is evident that the changes are associated with the surface temperature bands reported by Kuhn et al. [60]. Also, Woodard & Libbrecht [95] found a strong correlation between oscillation frequency changes and solar surface magnetic variations from monthly averages of their data. The origin of this behaviour, as well as the temporal variation of the frequencies is still ambiguous, but it appears clear that all these changes are consistent with a near surface perturbation.

The even-order splitting coefficients $a_{2k,l,n}$, seen in Eq. (63) can be fitted to the following formula obtained by Dziembowski & Goode [35]:

$$a_{2k,l,n} = a_{2k,l,n;\text{rot}} + C_{k,l} \frac{\gamma_k}{I_{l,n}}, \quad (70)$$

where $a_{2k,l,n;\text{rot}}$ represents the effect of centrifugal distortion which can be calculated following the treatment of Dziembowski & Goode [36]; $I_{l,n}$ is a measure of the modal inertia; $C_{k,l}$ is a constant which depends on the degree and on k , and γ_k is the asphericity coefficients which is directly related to the distortion described by the $P_{2k}(\mu)$ Legendre polynomial. The $P_2(\mu)$ term corresponds to a quadrupolar distortion (the oblateness), while $P_4(\mu)$ is the hexadecapole shape term and so on.

Dziembowski et al. in [37] have studied the behaviour of the even splitting coefficients $a_{2k,l,n}$ of p modes, obtained by observations covering almost all the period during the past 11 years cycle. In Fig. 17, taken from [37], there are shown the mean values of the γ_k coefficients as obtained by observations from various instruments, which include BBSO for the period 1986–1990, LOWL for the year 1994 and SOHO/MDI for the period 1996–1997. The variation of the asphericity coefficients is compared in Fig. 17 with the monthly averages of smoothed sunspot numbers. Clearly, the BBSO data of 1988 and 1989 give the largest magnitudes of γ_1 , γ_2 and γ_3 , and this corresponds to the first half of the previous sunspot maximum. In years of high activity all three coefficients are substantial and change rapidly, while during low magnetic activity their value is roughly zero. In particular the asphericity appears more pronounced in period of high activity when it happens that $P_2(\mu)$ and $P_4(\mu)$ distortions decrease while the $P_6(\mu)$ distortion increases. This can be translated in the fact that the Sun assumes a shape which varies from simply oblate to complicated asphericity according to the magnetic cycle.

This interesting conclusion has been confirmed by Howe et al. [52], which analyzed data obtained by the GONG network during the period 1995–1998.

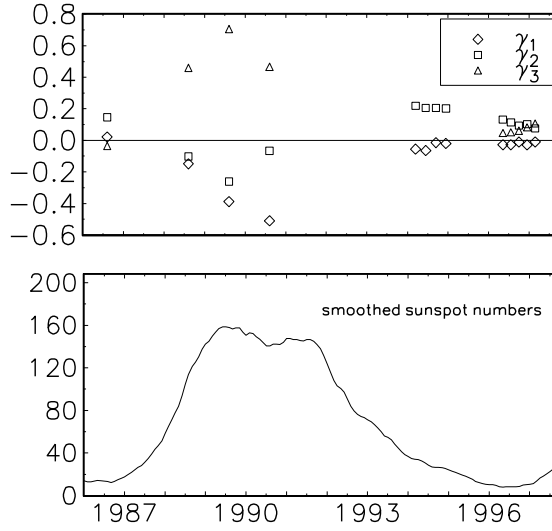


Fig. 17. The lower panel is a smoothed monthly average of the sunspot number covering the time since the 1986 activity minimum. The upper panel is a combination of γ 's derived from BBSO (1986–90), LOWL (1994) and SOHO/MDI (1996–97) data. The errors in the γ 's are smaller than the symbols used to represent their values [37]

They also observed that the temporal variation of the a_{2k} -coefficients is strongly correlated with the latitudinal distribution of the surface magnetic activity.

The behaviour of the γ 's as function of the frequency [37] yields, also, information about the sources of the solar distortion reflected in the even- a coefficients. It is well-known that p modes sample the region just above their inner turning points. Recently, Dziembowski et al. [38] found a significant aspherical distortion in the layer located at a depth ranging between 25 and 100 Mm. The perturbations seems to arise from a relative temperature increase of about 1.2×10^{-4} or from a magnetic perturbation, with $\langle B^2 \rangle \simeq (60 \text{ KG})^2$.

9 Concluding remarks

Helioseismology, through the very accurate identification of oscillation frequencies of acoustic and fundamental modes, has clearly demonstrated that the standard solar models reproduce the behaviour of the Sun with remarkably accuracy, consistent within 1 %.

Despite such overall success, this discipline has not yet exhausted its resources, since helioseismic results clearly suggest further refinements of the solar models.

The detailed structure of the convective zone and of the near-surface region is quite uncertain, since there remains substantial ambiguity associated with modelling the convective flux, taking into account the non-adiabatic effects, ex-

plaining the excitation and damping of the solar oscillations and defining an appropriate equation of state to describe the thermodynamic properties of the solar structure.

The attempts to restore the solar core conditions, up to now, have been contradictory too. In fact p modes (as opposed to gravity modes, g modes) are not very sensitive to the core of the Sun. This indicates the necessity of using more accurate low degree p-mode data and to continue to investigate for the presence of g modes.

In addition, there is still much work ahead in getting a detailed understanding of the Sun's rotation. Some rotational features like, for example, the temporal changes which occur near the base of the convective envelope have not been yet explained.

Finally, by studying the connection between the seismic and the global characteristics of the Sun, the challenge is to find the reason for the correlation between the variation of the Sun's shape and the magnetic solar cycle.

Ever more precise helioseismic observations from ground and space can help us to reconstruct the complete picture of the Sun and, finally, to solve the most discussed open questions in solar physics such as the solar neutrino problem, the history of the Sun's angular momentum, and the solar cycle generation mechanism, through the interaction of the convective motions with the rotation inside the Sun.

Recently, a new window has been opened on the astrophysics research: the possibility to study and to understand the behaviour of other stars by applying the tools and the techniques well developed and used in helioseismology. In fact, the success of helioseismology has spurred investigators to extend this diagnostic to other stars which may show multi-mode pulsations. Up to now, the seismological study of pulsating stars, known as *Asteroseismology*, has been hindered by the problem of mode identification since the oscillation amplitudes observed on the Sun (a few parts per million in flux) are too small to be detected in other stars with ground-based telescopes. To reach the required sensitivity and frequency resolution, several space experiments, MONS [54], COROT [81], MOST [66], will soon be devoted to the measurements of stellar oscillations. Thus, it is evident that asteroseismology represents the successive step in the evolution of the helioseismology research.

Acknowledgements

I thank the organizers of the *5eme Ecole d'Astrophysique solaire*, particularly J.P. Rozelot for an excellent and very enjoyable meeting. The work presented here was supported in part by the Danish National Research Foundation through its establishment of the Theoretical Astrophysics Center and in addition by the Formation Permanente du CNRS (France). I am very grateful to J. Christensen-Dalsgaard for his reading of an early version of this paper and for fruitful discussions and comments which have substantially improved this presentation.

References

1. C.W Allen: *Astrophysical Quantities*, 3rd edn. (Athlone, London 1976)
2. H.M. Antia: Mont. Not. Roy. Astron. Soc. **274**, 499 (1995)
3. H.M. Antia: Astron. Astrophys. **330**, 336 (1998)
4. H.M. Antia, S. Basu: Astron. Astrophys. Suppl. **107**, 421 (1994)
5. G.E. Backus, J.F. Gilbert: Geophys. J. Roy. Astron. Soc. **16**, 169 (1968)
6. G.E. Backus, J.F. Gilbert: Phil. Trans. Roy. Soc. Lond. **A266**, 123 (1970)
7. S. Basu, H.M. Antia: Mont. Not. Roy. Astron. Soc. **276**, 1402 (1995)
8. S. Basu, J. Christensen-Dalsgaard: Astron. Astrophys. **322**, L5 (1997)
9. S. Basu, J. Christensen-Dalsgaard, J. Schou, M.J. Thompson, S. Tomczyk: Astrophys. J. **460**, 1064 (1996)
10. S. Basu, W. Däppen, A. Nayfonov: Astrophys. J. **518**, 895 (1999)
11. T. Brown, J. Christensen-Dalsgaard: Astrophys. J. **500**, L195 (1998)
12. S. Chandrasekhar: Astrophys. J. **139**, 664 (1964)
13. W.J. Chaplin, J. Christensen-Dalsgaard, Y. Elsworth, R. Howe, G.R. Isaak, R.M. Larsen, R. New, J. Schou, M.J. Thompson, S. Tomczyk: Mont. Not. Roy. Astron. Soc. **308**, 405 (1999)
14. W.J. Chaplin, Y. Elsworth, R. Howe, G.R. Isaak, C.P. McLeod, B.A. Miller, R. New: Mont. Not. Roy. Astron. Soc. **280**, 849 (1996)
15. P. Charbonneau, J. Christensen-Dalsgaard, R. Henning, R.M. Larsen, J. Schou, M.J. Thompson, S. Tomczyk: Astrophys. J. **527**, 445 (1999)
16. J. Christensen-Dalsgaard: *Stellar oscillations*, 4th edn. (University of Aarhus, 1998)
17. J. Christensen-Dalsgaard, G. Berthomieu: ‘Theory of Solar Oscillations’. In: *Solar Interior and Atmosphere*, ed. by A.N. Cox, W.C. Livingston, M. Matthews, (University of Arizona Press, Tucson 1991) pp. 401–478
18. J. Christensen-Dalsgaard, W. Däppen, S.V. Ajukov, E.R. Anderson, H.M. Antia, S. Basu, V.A. Baturin, G. Berthomieu, B. Chaboyer, S.M. Chitre, A.N. Cox, P. Demarque, J. Donatowicz, W.A. Dziembowski, M. Gabriel, D.O. Gough, D.B. Guenther, J.A. Guzik, J.W. Harvey, F. Hill, G. Houdek, C.A. Iglesias, A.G. Kosovichev, J.W. Leibacher, O. Morel, C.R. Proffitt, J. Provost, J. Reiter, E.J. Rhodes, F.J. Rogers, I.W. Roxburgh, M.J. Thompson, R.K. Ulrich: Science **272**, 1286 (1996)
19. J. Christensen-Dalsgaard, T.L.Jr. Duvall, D.O. Gough, J.W. Harvey, E.J.Jr. Rhodes: Nature **315**, 378 (1985)
20. J. Christensen-Dalsgaard, J. Schou, M. Thompson: Mont. Not. Roy. Astron. Soc. **242**, 353 (1990)
21. D.D. Clayton: *Principles of Stellar Evolution and Nucleosynthesis* (McGraw-Hill, New York 1968)
22. T. Corbard, G. Berthomieu, J. Provost, P. Morel: Astron. Astrophys. **330**, 1149 (1998)
23. T.G. Cowling: Mont. Not. Roy. Astron. Soc. **101**, 367 (1941)
24. J.P. Cox, R.T. Giuli: *Principles of stellar structure* (Gordon and Breach, New York 1968)
25. A.N. Cox, J.A. Guzik, R.B. Kidman: Astrophys. J. **342**, 1187 (1989)
26. I.J.D. Craig, J.C. Brown: *Inverse problems in astronomy: a guide to inversion strategies for remotely sensed data* (Adam Hilger, Bristol 1986)
27. W. Däppen, D.O. Gough, A.G. Kosovichev, A.G. Thompson: ‘A new inversion for the hydrostatic stratification of the Sun’. In: *Challenges to theories of the structure of moderate -mass stars*, Lecture Notes in Physics, **388**, ed. by D.O. Gough, J. Toomre, (Springer, Heidelberg 1991) pp. 111–120

28. F.L. Deubner: *Astron. Astrophys.* **44**, 371 (1975)
29. F.L. Deubner, D.O. Gough: *Ann. Rev. Astron. Astrophys.* **22**, 593 (1984)
30. M.P. Di Mauro: 'The potential of helioseismic data: revealing new details of the internal structure'. In: *2nd Meeting about Solar Research in Italy, L'Aquila, July 3-5, 2000*, Mem. Soc. Astron. Italiana, in press
31. M.P. Di Mauro, J. Christensen-Dalsgaard: 'New inferences of the Sun by high degree modes: the external layers and the equation of state'. In: *Recent Insights into the Physics of the Sun and Heliosphere - Highlights from SOHO and Other Space Missions IAU Symposium No. 203, Manchester, England August 2000*, ed. by P. Brekke, B. Fleck, and J.B. Gurman, in press
32. M.P. Di Mauro, W.A. Dziembowski: 'Differential Rotation of the solar interior: New Helioseismic results by inversion of the SOI-MDI/SOHO data'. In: *Recent Results of The Italian Solar Research, Rome, 18-20 March 1998*, ed. by I. Ermolli, F. Berrilli, B. Caccin, Mem. Soc. Astron. Italiana **Vol. 69/3**, pp. 559-562
33. M.P. Di Mauro, W.A. Dziembowski, L. Paternò: 'Rotation of the Solar Interior: New Results by helioseismic data inversions'. In: *Structure and Dynamics of the Interior of the Sun and Sun-like Stars SOHO6/GONG98 Workshop, Boston, USA, 1-4 June 1998*, ESA SP-418 ed. by S.G. Korzennik, A. Wilson (ESA Publications Division, Noordwijk 1998) pp. 759-762
34. T.L.Jr. Duvall: *Nature* **300**, 242 (1982)
35. W.A. Dziembowski, P.R. Goode: *Astrophys. J.* **376**, 782 (1991)
36. W.A. Dziembowski, P.R. Goode: *Astrophys. J.* **394**, 670 (1992)
37. W.A. Dziembowski, P.R. Goode, M.P. Di Mauro, A.G. Kosovichev and J. Schou: *Astrophys. J.* **509**, 456 (1998)
38. W.A. Dziembowski, P.R. Goode, A.G. Kosovichev and J. Schou: *Astrophys. J.* **537**, 1026 (2000)
39. W.A. Dziembowski, P.R. Goode, A.A. Pamyatnykh, R. Sienkiewicz: *Astrophys. J.* **432**, 417 (1994)
40. W.A. Dziembowski, A.A. Pamyatnykh, R. Sienkiewicz: *Mont. Not. Roy. Astron. Soc.* **244**, 542 (1990)
41. W.A. Dziembowski, A.A. Pamyatnykh, R. Sienkiewicz: *Mont. Not. Roy. Astron. Soc.* **249**, 542 (1991)
42. W.A. Dziembowski, A.A. Pamyatnykh, R. Sienkiewicz: *Acta Astron.* **42**, 5 (1992)
43. J.R. Elliott, A.G. Kosovichev: *Astrophys. J.* **500**, L199 (1998)
44. A. Gabriel, S. Turck-Chièze, R.A. García, P.L. Pallé, P. Boumier, S. Thiery, G. Grec, R.K. Ulrich, L. Bertello, T. Roca Cortés, J.-M. Robillot: 'Search for g-mode frequencies in the GOLF oscillation spectrum'. In: *Structure and Dynamics of the Interior of the Sun and Sun-like Stars, Soho6/Gong98 Workshop, Boston, USA, 1-4 June 1998*, ESA SP-418, ed. by S.G. Korzennik, A. Wilson (ESA Publications Division, Noordwijk 1998) pp. 61-66
45. E. Gavryuseva, V. Gavryusev, M.P. Di Mauro: 'Rotational Split of Solar Acoustic Modes from GONG Experiment'. In: *Structure and Dynamics of the Interior of the Sun and Sun-like Stars, SOHO6/GONG 98 Workshop, Boston, USA, 1-4 June 1998* ESA SP-418, ed. by S.G. Korzennik, A. Wilson (ESA Publications Division, Noordwijk 1998) pp. 193-198
46. D.O. Gough: 'Towards a solar model'. In: *Conference on Oscillations as a Probe of the Sun's Interior, Catania, Italy, June 20-24, 1983* Mem. Soc. Astron. Italiana **55**, 13 (1984)
47. D.O. Gough: 'Testing solar models: the inverse problem'. In: *The structure of the Sun*, ed. by T. Roca Cortés, F. Sánchez, (Cambridge University Press, Cambridge 1996)

48. D.O. Gough, M.J. Thompson: ‘The inversion problem’. In: *Solar Interior and Atmosphere*, ed. by A.N. Cox, W.C. Livingston, M. Matthews, (University of Arizona Press, Tucson 1991) pp. 519–561
49. D.O. Gough, S.V. Vorontsov: *Mont. Not. Roy. Astron. Soc.* **273**, 573 (1995)
50. N. Grevesse, A. Noels: ‘Cosmic abundances of the elements’. In: *Origin and evolution of the Elements*, ed. by N. Prantzos, E. Vangioni-Flam & M. Cassé (Cambridge Univ. Press, Cambridge 1993) pp. 15–25
51. R. Hove, J. Christensen-Dalsgaard, F. Hill, R.W. Komm, R.M. Larsen, J. Schou, M.J. Thompson, J. Toomre: *Science* **287**, 2456
52. R. Hove, R.W. Komm, F. Hill: *Astrophys. J.* **524**, 1084 (1999)
53. R. Kippenhahn, A. Weigert: *Stellar Structure and Evolution*, 2nd edn. (Springer, Berlin, Heidelberg 1991)
54. H. Kijeldsen, T.R. Bedding, J. Christensen-Dalsgaard: ‘MONS: Measuring Oscillations in Nearby Stars’. In: *The Impact of Large-Scale Surveys on Pulsating Star Research, IAU Colloquium 176*, ASP Conference Series Vol. **203**, ed. by L. Szabados and D. Kurtz., p. 73 (2000)
55. A.G. Kosovichev: *Mont. Not. Roy. Astron. Soc.* **265**, 1053 (1993)
56. A.G. Kosovichev, J. Christensen-Dalsgaard, W. Däppen, W.A. Dziembowski, D.O. Gough, M.J. Thompson: *Mont. Not. Roy. Astron. Soc.* **259**, 536 (1992)
57. A.G. Kosovichev: *Bull. Astron. Soc. India*, **24**, 355 (1997)
58. J.R. Kuhn: *Astrophys. J.* **331**, L131 (1988)
59. J.R. Kuhn: *Astrophys. J.* **339**, L45 (1989)
60. J.R. Kuhn, K.G. Libbrecht, R.H. Dicke: *Science* **242**, 908 (1996)
61. M. Lazrek, A. Pantel, E. Fossat, B. Gelly, F.X. Schmider, D. Fierry-Fraillon, G. Grec, S. Loudagh, S. Ehgamberdiev, I. Khamitov, J.T. Hoeksema, P.L. Pallè, C. Régulo: *Sol. Phys.* **166**, 1 (1996)
62. J.W. Leibacher, R.F. Stein: *Astrophys. Lett.* **7**, 191 (1971)
63. R.B. Leighton, R.W. Noyes, G.W. Simon: *Astrophys. J.* **135**, 474 (1962)
64. K.G. Libbrecht: *Space Sci. Rev.* **47**, 275 (1988)
65. K.G. Libbrecht, M.F. Woodard: *Nature* **345**, 779 (1990)
66. J.M. Matthews: ‘Asteroseismology from Space: Getting the MOST Science for the least money’. In: *Structure and Dynamics of the Interior of the Sun and Sun-like Stars, SOHO6/GONG98 Workshop, Boston, USA, 1–4 June 1998* ESA SP-418, ed. by S.G. Korzennik, A. Wilson (ESA Publications Division, Noordwijk 1998) pp. 395–398
67. D. Mihalas, W. Däppen, D.G. Hummer: *Astrophys. J.* **331**, 815 (1988)
68. R.W. Noyes, R.B. Leighton: *Astrophys. J.* **138**, 631 (1963)
69. L. Paternò, S. Sofia, M.P. Di Mauro: *Astron. Astrophys.* **314**, 940 (1996)
70. R.L. Parker: *Ann. Rev. Earth Planet. Sci.* **5**, 35 (1977)
71. D.L. Phillips: *J. Assoc. Comput. Mech.* **9**, 84 (1962)
72. F.P. Pijpers: *Mont. Not. Roy. Astron. Soc.* **297**, L76 (1998)
73. F.P. Pijpers, M.J. Thompson: *Astron. Astrophys.* **262**, L33 (1992)
74. F.P. Pijpers, M.J. Thompson: *Astron. Astrophys.* **281**, 231 (1994)
75. E.J. Rhodes, J. Reiter, A.G. Kosovichev, J. Schou, P.H. Scherrer: ‘Initial SOI/MDI High-Degree Frequencies and Frequency Splittings’. In: *Structure and Dynamics of the Interior of the Sun and Sun-like Stars, SOHO6/GONG98 Workshop, Boston, USA, 1–4 June 1998*, ESA SP-418, ed. by S.G. Korzennik, A. Wilson (ESA Publications Division, Noordwijk 1998) pp. 73–82
76. O. Richard, S. Vauclair, C. Charbonnel, W.A. Dziembowski: *Astron. Astrophys.* **312**, 1000 (1996)

77. O. Richard, W.A. Dziembowski, R. Sienkiewicz, P.R. Goode: *Astron. Astrophys.* **338**, 756 (1998)
78. M.H. Ritzwoller, E.M. Lavelly: *Astrophys. J.* **403**, 810 (1991)
79. T. Roca Cortés, M. Lazrek, L. Bertello, R.A. García, S. Thiery, F. Baudin, P. Boumier, V. Gavryusev, S. Turck-Chièze, A.H. Gabriel, C. Régulo, R.K. Ulrich, G. Grec, J.-M. Robillot: ‘The Solar acoustic Spectrum as seen by GOLF. III Asymmetries, resonant Frequencies and Splittings’. In: *Structure and Dynamics of the Interior of the Sun and Sun-like Stars, SOHO6/GONG98 Workshop, Boston, USA, 1–4 June 1998*, ESA SP-418, ed. by S.G. Korzenik, A. Wilson (ESA Publications Division, Noordwijk 1998) pp. 329–334
80. F.J. Rogers, F.J. Swenson, C.A. Iglesias: *Astrophys. J.* **456**, 902 (1996)
81. I.W. Roxburgh: *Astrophys. and Space Sci.* **261**, 1, 19
82. P.H. Scherrer, R.S. Bogart, R.I. Bush, J.T. Hoeksema, A.G. Kosovichev, J. Schou, W. Rosenberg, L. Springer, T.D. Tarbell, A. Title, C.J. Wolfson, I. Zayer and the MDI engineering team: *Solar. Phys.* **162**, 129 (1995)
83. J. Schou: ‘Observations of Medium-and High-Degree Modes: Methods and sand-Traps’. In: *Structure and Dynamics of the Interior of the Sun and Sun-like Stars, SOHO6/GONG98 Workshop, Boston, USA, 1–4 June 1998*, ESA SP-418, ed. by S.G. Korzenik and A. Wilson, (ESA Publications Division, Noordwijk 1998) pp. 47–52
84. J. Schou, J. Christensen-Dalsgaard, M.J. Thompson: *Astrophys. J.* **433**, 389 (1994)
85. J. Schou, A.G. Kosovichev, P.R. Goode, W.A. Dziembowski: *Astrophys. J.* **489**, 197 (1997)
86. J. Schou, H.M. Antia, S. Basu, R.S. Bogart, R.I. Bush, S.M. Chitre, J. Christensen-Dalsgaard, M.P. Di Mauro, W.A. Dziembowski, A. Eff-Darwich, D.O. Gough, D.A. Haber, J.T. Hoeksema, R. Howe, S.G. Korzenik, A.G. Kosovichev, R.M. Larsen, F.P. Pijpers, P.H. Scherrer, T. Sekii, T.D. Tarbell, A.M. Title, M.J. Thompson, J. Toomre: *Astrophys. J.* **505**, 1 (1998)
87. M. Schwarzschild: *Structure and Evolution of the Stars*, 2nd edn. (Princeton University Press, Princeton 1958)
88. T. Sekii: ‘Internal Solar Rotation’. In: *Sounding Solar and Stellar Interiors* IAU Symp. No. 181, ed. by J. Provost and F.-X. Schmider (Kluwer Academic Publishers, Dordrecht 1997) pp. 189–202
89. E.A. Spiegel, J.P. Zahn: *Astron. Astrophys.* **265**, 106 (1992)
90. A. Tarantola: *Inverse Problem Theory: Methods for data fitting and model parameter estimations*, (Elsevier, Amsterdam 1987)
91. A.N. Tikhonov: *Sov. Maths. Dokl.* **4**, 1035 (1963)
92. R.K. Ulrich: *Astrophys. J.* **162**, 993 (1970)
93. W. Unno, Y. Osaki, H. Ando, H. Shibahashi: *Nonradial Oscillations of Stars*, 2nd edn. (University of Tokyo Press, Tokyo 1989)
94. R.C. Willson, H.S. Hudson: *Nature* **332**, 810 (1988)
95. M.F. Woodard, K.G. Libbrecht: *Astrophys. J.* **374**, L61 (1991)